



Chikungunya Virus Replication Rate Determines the Capacity of Crossing Tissue Barriers in Mosquitoes

Fernando Merwaiss, Claudia V Filomatori, Yasutsugu Susuki, Eugenia S Bardossy, Diego E Alvarez, María-Carla Saleh

► To cite this version:

Fernando Merwaiss, Claudia V Filomatori, Yasutsugu Susuki, Eugenia S Bardossy, Diego E Alvarez, et al.. Chikungunya Virus Replication Rate Determines the Capacity of Crossing Tissue Barriers in Mosquitoes. *Journal of Virology*, 2021, 95 (3), pp.e01956-20. 10.1128/JVI.01956-20 . pasteur-04086887

HAL Id: pasteur-04086887

<https://pasteur.hal.science/pasteur-04086887>

Submitted on 2 May 2023



HAL is a multi-disciplinary open access archive for the deposit and dissemination of scientific research documents, whether they are published or not. The documents may come from teaching and research institutions in France or abroad, or from public or private research centers.

L'archive ouverte pluridisciplinaire **HAL**, est destinée au dépôt et à la diffusion de documents scientifiques de niveau recherche, publiés ou non, émanant des établissements d'enseignement et de recherche français ou étrangers, des laboratoires publics ou privés.

Copyright



Chikungunya Virus Replication Rate Determines the Capacity of Crossing Tissue Barriers in Mosquitoes

Fernando Merwaiss,^{a,b} Claudia V. Filomatori,^a Yasutsugu Susuki,^b Eugenia S. Bardossy,^a  Diego E. Alvarez,^a  María-Carla Saleh^b

^aInstituto de Investigaciones Biotecnológicas, Universidad Nacional de San Martín, Buenos Aires, Argentina

^bInstitut Pasteur, Viruses and RNA Interference Unit, Centre National de la Recherche Scientifique UMR 3569, Paris, France

Diego E. Alvarez and María-Carla Saleh contributed equally.

ABSTRACT Chikungunya virus (CHIKV) is a reemerging and rapidly spreading pathogen transmitted by mosquitoes. The emergence of new epidemic variants of the virus is associated with genetic evolutionary traits, including duplication of repeated RNA elements in the 3' untranslated region (UTR) that seemingly favor transmission by mosquitoes. The transmission potential of a given variant results from a complex interplay between virus populations and anatomical tissue barriers in the mosquito. Here, we used the wild-type CHIKV Caribbean strain and an engineered mutant harboring a deletion in the 3' UTR to dissect the interactions of virus variants with the anatomical barriers that impede transmission during the replication cycle of the virus in *Aedes* mosquitoes. Compared to the 3'-UTR mutant, we observed that the wild-type virus had a short extrinsic incubation period (EIP) after an infectious blood meal and was expectorated into mosquito saliva much more efficiently. We found that high viral titers in the midgut are not sufficient to escape the midgut escape barrier. Rather, viral replication kinetics play a crucial role in determining midgut escape and the transmission ability of CHIKV. Finally, competition tests in mosquitoes coinfecting with wild-type and mutant viruses revealed that both viruses successfully colonized the midgut, but wild-type viruses effectively displaced mutant viruses during systemic infection due to their greater efficiency of escaping from the midgut into secondary tissues. Overall, our results uncover a link between CHIKV replication kinetics and the effect of bottlenecks on population diversity, as slowly replicating variants are less able to overcome the midgut escape barrier.

IMPORTANCE It is well established that selective pressures in mosquito vectors impose population bottlenecks for arboviruses. Here, we used a CHIKV Caribbean lineage mutant carrying a deletion in the 3' UTR to study host-virus interactions *in vivo* in the epidemic mosquito vector *Aedes aegypti*. We found that the mutant virus had a delayed replication rate in mosquitoes, which lengthened the extrinsic incubation period (EIP) and reduced fitness relative to the wild-type virus. As a result, the mutant virus displayed a reduced capacity to cross anatomical barriers during the infection cycle in mosquitoes, thus reducing the virus transmission rate. Our findings show how selective pressures act on CHIKV noncoding regions to select variants with shorter EIPs that are preferentially transmitted by the mosquito vector.

KEYWORDS 3' UTR, alphavirus, arthropod vectors, bottlenecks, extrinsic incubation period

Chikungunya virus (CHIKV) is an arthropod-borne virus that after 60 years of exclusive circulation in Asia and Africa has recently spread into Europe and America, producing about 1.7 million infections (1–5). CHIKV infection has thus emerged as a

Citation Merwaiss F, Filomatori CV, Susuki Y, Bardossy ES, Alvarez DE, Saleh M-C. 2021. Chikungunya virus replication rate determines the capacity of crossing tissue barriers in mosquitoes. *J Virol* 95:e01956-20. <https://doi.org/10.1128/JVI.01956-20>.

Editor Susana López, Instituto de Biotecnología/UNAM

Copyright © 2021 American Society for Microbiology. All Rights Reserved.

Address correspondence to Diego E. Alvarez, dalvarez@iib.unsam.edu.ar, or María-Carla Saleh, carla.saleh@pasteur.fr.

Received 30 September 2020

Accepted 27 October 2020

Accepted manuscript posted online 4 November 2020

Published 13 January 2021

major public health concern since it may affect a large proportion of the population within an outbreak area (6). CHIKV infections are usually nonfatal and resolve over time, but they cause considerable pain, distress, and anxiety as well as a significant economic burden due to severe clinical manifestations (7–9). There is no commercially available vaccine against CHIKV, and intervention efforts during outbreaks focus on preventing mosquito exposure and inhibiting local mosquito population growth (10, 11).

CHIKV cycles between mosquito and human hosts and has evolved strategies that allow maintenance of efficient replication in these two disparate host environments. Research efforts have focused on the identification of viral genome sequences that determine the virus host range (12). The CHIKV genome is a single-stranded positive-sense RNA of 11 to 12 kb that carries a 3′ untranslated region (UTR) containing 50- to 80-nucleotide (nt)-long sequence repetitions referred to as direct repeats (13, 14) that change in copy number among viral strains (15–17). Evidence shows that the 3′ UTR is subjected to conflicting selective pressures in mammalian and mosquito hosts and that duplicated direct repeats are maintained in nature due to positive selection in the mosquito host (17). The Caribbean strains bear the longest 3′ UTRs among CHIKV lineages and display 5 copies of direct repeats. Previous work from our group showed that virus replication in mammalian cells results in the emergence of variants carrying large 3′-UTR deletions that are cleared in mosquitoes (18). In addition, Chen et al. reported that for the Asian CHIKV strain, an intact 3′ UTR provides a selective advantage in mosquitoes over a virus with a shorter 3′ UTR, as viruses with intact 3′ UTRs prevailed in the heads of mosquitoes 10 days after mixed infections (16). While *in vitro* studies demonstrate delayed replication rates of 3′-UTR deletion mutants in C6/36 mosquito cells, a detailed investigation of the relevance of CHIKV replication kinetics in mosquitoes *in vivo* is still lacking. Moreover, consequences on transmission dynamics for viral variants with delayed growth have not yet been explored (19).

The transmission efficiency (TE) and the extrinsic incubation period (EIP) are two common indexes used to describe the interaction between viruses and their vectors. While the first one is related to the ability of the pathogen to be successfully transmitted to another susceptible host, the second one defines the interval of time for this infectious cycle to be completed (20, 21). Both parameters are highly dependent on four anatomical barriers or bottlenecks that viruses must cross within the mosquito in order to be transmitted (22–24). The first barrier is determined by the capacity of the virus to infect and replicate in midgut epithelial cells of the mosquito after a blood meal (midgut infection barrier). Once it has successfully established a midgut infection, escape from the midgut imposes a barrier for the virus to disseminate through the hemolymph to secondary organs and peripheral tissues such as the fat body and trachea. The inability to disseminate at this step could result from defects in the release of virions from midgut epithelial cells (midgut escape barrier). The next anatomical barrier to infection occurs at the end of the dissemination process when the virus has to reach the salivary glands (salivary gland infection barrier). Finally, in order to be successfully transmitted, viruses must replicate efficiently inside salivary glands to be released into the saliva, which is injected into a human host when the mosquito takes the next blood meal (salivary gland escape barrier). For CHIKV, the salivary gland escape barrier has a very strong impact on virus transmission efficiency (25–27).

In this work, we addressed the relationship between CHIKV replication kinetics and its capacity to overcome successive physiological barriers and complete a replication cycle in mosquitoes in order to be successfully transmitted. We gained insight into barriers to arbovirus transmission using an engineered variant of the Caribbean strain of CHIKV bearing a deletion of the first 500 nt of the 3′ UTR as a tool. Our data show that delayed growth kinetics in *Aedes* mosquitoes resulted in an extended EIP, which in turn compromised transmission efficiency. We found that this effect on transmission is associated with a severe bottleneck during escape from the midgut and, to a lesser extent, impaired secretion into saliva. In addition, virus competition assays in mosquitoes showing that small amounts of fast-replicating viral variants were able to displace

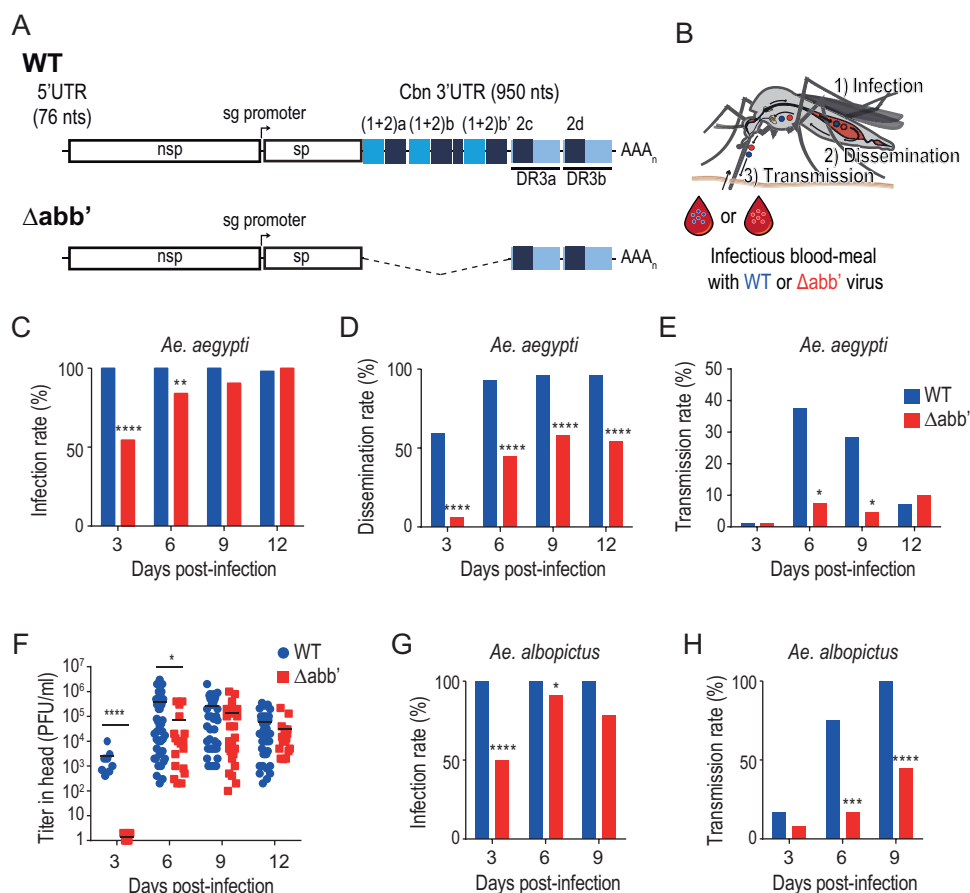


FIG 1 Extrinsic incubation period of wild-type and $\Delta abb'$ mutant CHIKVs in *Aedes* mosquitoes. (A) Schematic representation of the genomes of wild-type (WT) and $\Delta abb'$ mutant viruses. The $\Delta abb'$ mutant bears a deletion of the first 500 nucleotides of the 3' UTR. (B) Extrinsic incubation period of WT and $\Delta abb'$ CHIKVs. Mosquitoes were blood fed with 10^6 PFU/ml of WT or $\Delta abb'$ mutant viruses, and the presence of virus was analyzed in the body (as a proxy of the infection rate), the head (as a proxy of the rate of dissemination to salivary glands), and the saliva (indicative of the transmission rate) at different times postinfection. (C to E) Bar graphs showing infection, dissemination, and transmission rates of WT and $\Delta abb'$ viruses in infected *Aedes aegypti* mosquitoes. (C) The infection rate was calculated as the percentage of infected mosquito bodies at each time point. (D) The dissemination rate was scored as the number of infected mosquito heads over the number of infected bodies. (E) The transmission rate was measured as the ratio between the number of mosquito saliva samples with detectable virus and the number of mosquitoes in which dissemination was successful. Bars for infection, dissemination, and transmission rates represent cumulative data from two independent experiments ($n = 48$). Data were analyzed by Fisher's exact test. (F) Dot plot showing mean viral titers and standard deviations (SD) of WT and $\Delta abb'$ viruses in the heads of infected mosquitoes. Infectious virus titers were measured in the heads of mosquitoes displaying positive CPE at each time point by plaque assays in Vero cells. Data represent the titers in individual mosquitoes. Statistics were performed by a Mann-Whitney U test. (G and H) Infection and dissemination rates in *Aedes albopictus* mosquitoes. Bar graphs for infection (G) and dissemination (H) rates are shown ($n = 24$). Data were analyzed by Fisher's exact test.

slow-replicating viruses in disseminated tissues provide novel insight into how mosquito bottlenecks restrict arbovirus diversity.

RESULTS

Mosquito replication cycle of wild-type and 3'-UTR deletion mutant viruses. To gain insight into the mosquito cycle of the Caribbean CHIKV strain in its epidemic vector, we used *Aedes aegypti* mosquito infections to determine the EIPs of wild-type (WT) virus and an engineered 3'-UTR deletion mutant (referred to here as $\Delta abb'$) that has been previously described to show impaired growth rates in mosquito cells *in vitro* (18) (Fig. 1A). Laboratory colonies of *Aedes aegypti* mosquitoes were fed with an infectious blood meal containing 10^6 PFU/ml of wild-type or $\Delta abb'$ mutant virus. At 3, 6, 9, and 12 days after the blood meal, we analyzed the presence of each virus in the

TABLE 1 Infection, dissemination, and transmission rates (percentages) estimated on different days after exposure of *A. aegypti* to the CHIKV wild-type or Δ abb' mutant strain^a

Day postinfection	CHIKV wild type			CHIKV Δ abb'		
	IR [no. of mosquitoes (%)]	DR [no. of mosquitoes (%)]	TR [no. of mosquitoes (%)]	IR [no. of mosquitoes (%)]	DR [no. of mosquitoes (%)]	TR [no. of mosquitoes (%)]
3	48 (100)	28 (58)	0 (0)	48 (55)	2 (6)	0 (0)
6	48 (100)	45 (93)	17 (38)	48 (84)	18 (45)	1 (7)
9	48 (100)	46 (96)	13 (29)	48 (91)	25 (58)	1 (4)
12	48 (98)	45 (96)	3 (7)	48 (100)	26 (54)	2 (10)

^aAbbreviations: IR, infection rate; DR, dissemination rate; TR, transmission rate.

body (as a proxy of the infection rate [IR]), in the head (as a proxy of dissemination rate [DR] to salivary glands) (28–30), and in the saliva (indicative of the transmission rate [TR]) in individual mosquitoes (Fig. 1B). For each virus, the infection rate was estimated as the percentage of mosquitoes with infectious viruses in their bodies (Fig. 1C), measured by the development of cytopathic effect (CPE) on Vero cells inoculated with whole-body extracts. At day 3, we observed that 100% of the engorged mosquitoes were infected with the wild-type virus, while only 50% of the mosquitoes exposed to the mutant virus became infected. Eventually, infection with the mutant virus progressed, and the whole pool of mosquitoes was infected by day 12. This result indicates that the Δ abb' mutant has no impediment in crossing the midgut infection barrier. Therefore, differences in the infection rates at short times after blood feeding rather reflect the lower growth rate of the mutant than of the wild type, resulting in longer times to reach the threshold level to be detected by our method. Next, we determined the dissemination rate, i.e., the ratio between the number of mosquito heads with detectable virus and the number of infected mosquitoes (Fig. 1D). The results showed a 50% dissemination rate for the wild type at day 3 and a 100% dissemination rate by day 6. In contrast, the Δ abb' virus was detected in the heads of infected mosquitoes only after 6 days, and even at later time points, it reached the head in no more than 50% of the individuals, pointing to a defect at a stage between colonization of the midgut and arrival to salivary glands. Finally, we measured the transmission rate, i.e., the ratio between the number of mosquito saliva specimens with detectable virus and the number of mosquitoes with disseminated infection (Fig. 1E). The transmission rate peaked at almost 40% for the wild type at day 6 and decreased by day 9. In contrast, Δ abb' CHIKV reached maximum transmission at day 12, with a rate of only 10%. For both dissemination and transmission rates, we used the cytopathic effect assay to score infection as it is informative of the nature of the infectivity of the virus in the disseminated tissues and, importantly, of the virus expectorated into saliva, respectively. As noted above, it may be possible that dissemination and transmission rates are underestimated compared to those determined by molecular methods because of the limit of detection of the assay. However, as opposed to the increase observed in the infection rate of the mutant virus, dissemination rates did not increase over the course of the experiment (compare days 6, 9, and 12 in Fig. 1D), suggesting that the mutant virus likely encounters a midgut escape barrier to infection. The results obtained for the wild-type transmission rate are similar to those in previous reports and show that the salivary gland entry and exit barriers impose the greatest limiting effect for transmission in nature (25, 26, 31). Infection, dissemination, and transmission rates of wild-type and Δ abb' viruses are summarized in Table 1.

In order to determine whether the decreased dissemination rate of the mutant is accompanied by lower viral titers in disseminated tissues, we measured the viral titers of wild-type and Δ abb' viruses in mosquito heads at different times postinfection (Fig. 1F). Consistent with the estimates of dissemination rates, the wild-type virus reached an average titer of 2×10^3 PFU/ml at day 3, while at this time point, mutant viruses were not detectable. However, as soon as infection disseminated at 6 days postinfection, the mutant virus reached viral titers comparable to those of the wild type. Therefore, the

defect in transmission is likely related to a growth delay rather than to a defect to reach high viral titers.

To evaluate whether this phenomenon extends to other vector species of CHIKV, the same experiment was performed by infecting *Aedes albopictus* mosquitoes. Estimates of infection and dissemination rates are presented in Fig. 1G and H. The results recapitulated our observations with *A. aegypti* mosquitoes, underscoring the role of viral replication kinetics in viral dissemination and subsequent transmission, regardless of the mosquito species.

Together, these data showed that similar to replication in cell culture, the mutant virus has a low replication rate at the site of colonization (i.e., mosquito midguts) that results in decreased abilities to disseminate as well as to be secreted into the mosquito saliva compared to the wild-type virus. This defect is also reflected in a longer EIP, defined as a quantitative trait of the mosquito population instead of a threshold time point at which the first mosquito becomes infectious (29).

Deficient dissemination of Δ abb' mutant virus is due to a defect to cross the midgut escape barrier. The delayed EIP of the Δ abb' mutant virus could reflect a problem of the virus either to leave midgut at the beginning of the infection or to spread through the hemolymph and reach secondary organs during dissemination. To differentiate between these two possibilities, we assessed infection rates and viral titers of wild-type or Δ abb' CHIKV in the midgut and carcass (i.e., the rest of the body after removing the midgut) of mosquitoes from days 2 to 8 after infectious blood feeding (Fig. 2A). Similar to the EIP, both viruses eventually reached almost a 100% rate of infection of midguts (day 2 versus day 6 for wild-type and mutant viruses, respectively), indicating efficient colonization of the midgut (Fig. 2B). Mean viral titers in the midgut were significantly lower for the mutant at early time points, and as of day 6, both viruses reached comparable titers (Fig. 2C), indicating delayed replication rates of Δ abb' compared to the wild type. The rate of carcass infection was used as a proxy for the ability to escape from the midgut and spread in the infected mosquito. The results showed that the mutant virus was detected in carcasses later than the wild type and failed to infect the carcass in half of the individuals (Fig. 2D), pointing to a defect in escape from the midgut. Similar to midgut viral titers, carcass titers were significantly lower for the mutant than for the wild-type virus at earlier times after infection. Despite the delayed replication kinetics, at day 8, both viruses reached comparable titers (Fig. 2E). Finally, we analyzed paired viral titers in the midgut and carcass of each individual as of the fourth day postinfection. Viral titers in the midgut were higher than 10^4 PFU/ml in 100% of mosquitoes infected with the wild-type virus, and in 96% of them, viral dissemination to the carcass was successful (Fig. 2F). In the case of mosquitoes infected with the mutant virus, although there was a slight drop in the number of individuals with midgut titers of $>10^4$ PFU/ml (89% of the analyzed mosquitoes), the virus was able to cross the midgut escape barrier in only 46% of these individuals (Fig. 2G). A possible interpretation of this result is that reaching a threshold value for viral titers in the midgut is necessary but not sufficient to guarantee successful dissemination. In addition to a threshold titer, a "window of opportunity" may define a timing effect that determines the ability to escape the midgut barrier (32). To test this hypothesis, we repeated the experiment using five-times-higher viral titers in the blood meal to increase the virus input in midgut cells (Fig. 3). We reasoned that increasing the viral titer in the input would allow the mutant to reach threshold titers earlier in the mosquito cycle and that it would favor escaping the midgut (33). Figure 3A shows that both viruses infected midguts at similar rates. In contrast to infections with a low input, infections with higher doses disseminated into the carcass as of day 2 for both viruses, and differences in dissemination rates disappeared at day 8 (Fig. 3C). Analysis of paired midgut and carcass viral titers further confirmed the effect of the input on the ability of the mutant virus to disseminate; we found that Δ abb' CHIKV achieved successful dissemination in 70% of mosquitoes with midgut titers of $>10^4$ PFU/ml (Fig. 3F). Thus, it appears that the delay to reach this threshold titer negatively impacted viral dissemination of the mutant, likely due to an impairment in overcoming the midgut escape

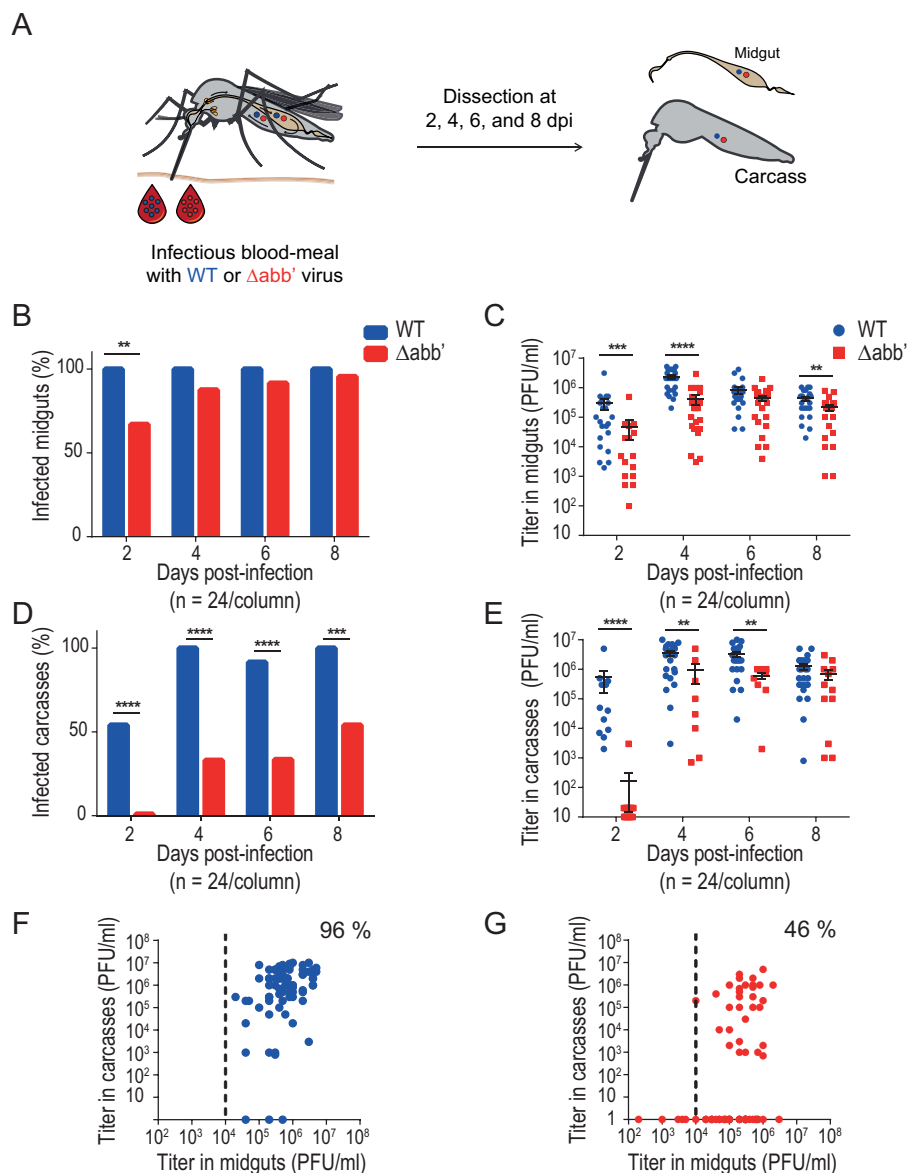


FIG 2 $\Delta abb'$ mutant CHIKV is impaired in escaping the midgut. (A) Midgut escape barrier assay. Mosquitoes were blood fed with 10^6 PFU/ml of wild-type (WT) or $\Delta abb'$ mutant CHIKV and dissected from days 2 to 8 to separate midguts and carcasses. Infection rates and viral titers were measured in each sample. dpi, days postinfection. (B) Bar graph showing midgut infection rates. Data represent the percentages of infected mosquito midguts at each time point. (C) Dot plot showing mean viral titers and SD of WT and $\Delta abb'$ viruses in midguts of infected mosquitoes. Virus titers in midgut extracts scored positive by a CPE assay were measured by a plaque assay. Data represent titers of individual midguts. (D) Bar graph showing carcass infection rates. Data represent the percentages of infected carcasses at different times after blood feeding and reflect virus dissemination efficiencies. (E) Dot plot showing mean viral titers and SD of WT and $\Delta abb'$ viruses in carcasses of infected mosquitoes. Virus titers in carcass extracts were measured by plaque assays. Data represent titers in individual carcasses. (F and G) Scatterplots of viral titers in the midgut versus carcass for individual mosquitoes from the fourth to eighth days postinfection. The dotted line indicates the threshold titer needed to leave the midgut, which was set at 10^4 PFU/ml. The percentage of mosquitoes above this threshold with disseminated infection was measured for wild-type (F) and mutant (G) viruses. Statistics on infection rates were performed by Fisher's exact test on cumulative data ($n = 24$) from two independent experiments. Statistics on viral titers were performed by a Mann-Whitney U test.

barrier. In summary, these results indicate that the initial dose and viral replication kinetics have a strong effect on the ability of CHIKV to escape the midgut.

Deficiency in viral replication capacity also occurs in secondary tissues during dissemination. With the aim of assessing if the slow replication kinetics of the $\Delta abb'$

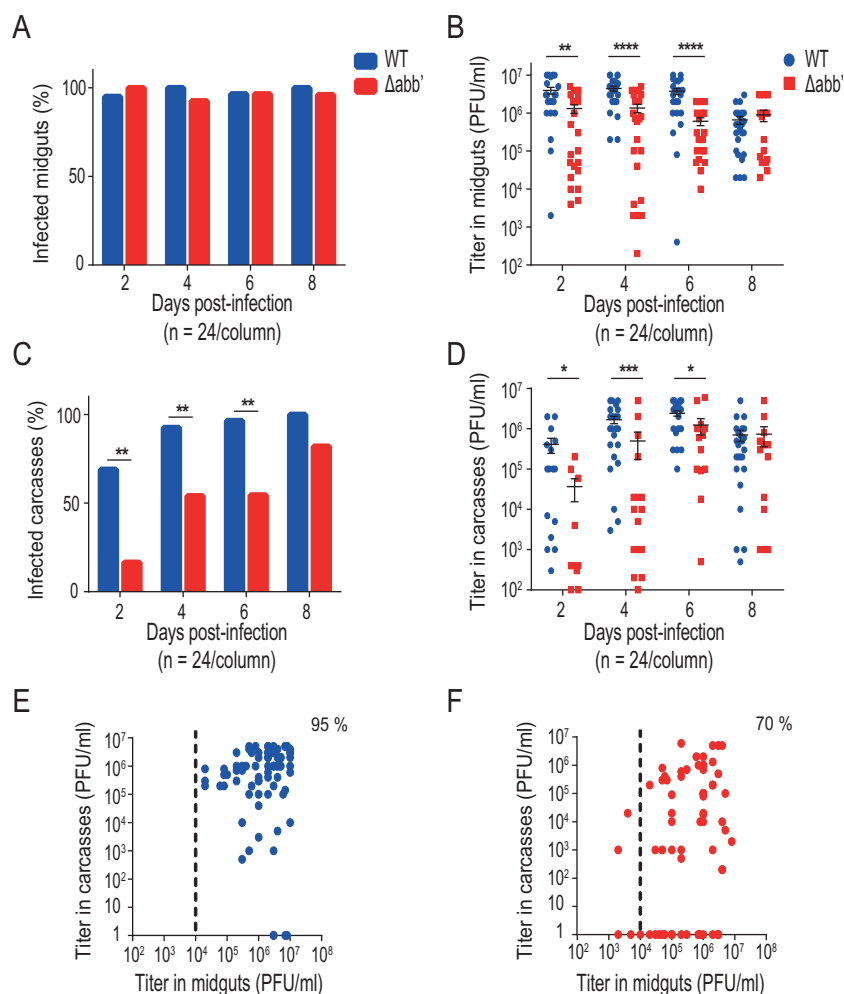


FIG 3 Increasing the infectious dose decreases the midgut escape barrier effect. Mosquitoes were blood fed with 5×10^6 PFU/ml wild-type (WT) or $\Delta abb'$ mutant CHIKV and dissected from days 2 to 8 to separate midguts and carcasses. Infection rates and viral titers were measured in each sample. (A) Bar graph showing midgut infection rates. (B) Dot plot showing mean viral titers and SD of WT and $\Delta abb'$ viruses in midguts of infected mosquitoes. (C) Bar graph showing carcass infection rates. (D) Dot plot showing mean viral titers and SD of WT and $\Delta abb'$ viruses in carcasses of infected mosquitoes. (E and F) Scatterplot of viral titers in the midgut versus carcass for wild type (E) and mutant (F) viruses. Statistics on infection rates were performed by Fisher's exact test on cumulative data ($n = 24$) from two independent experiments. Statistics on viral titers were performed by a Mann-Whitney U test.

virus impacts barriers other than the midgut escape barrier during the mosquito replication cycle, we infected mosquitoes through the intrathoracic route to bypass the first two barriers that occur during infectious blood feeding (i.e., the midgut infection and escape barriers) (Fig. 4A). Mosquitoes were intrathoracically injected with 2,500 PFU of the wild-type or $\Delta abb'$ mutant virus so that the initial viral titers in the mosquito hemolymph were the same for both viruses. Next, infection and transmission rates as well as viral titers in the body of infected mosquitoes were measured every 2 days. Mosquito infection rates, estimated as the presence of viruses in the body at different times postinjection, were 100% for both viruses at all tested time points (Fig. 4B). Virus titration in the bodies showed ~ 10 -fold-higher viral titers for the wild type than for the mutant at days 2 and 4, and as of day 6, both viruses showed the same titers (Fig. 4C). In turn, the overall trend of the transmission rate, estimated as the presence of viruses in the saliva, was slightly lower for the mutant than for the wild type (Fig. 4D). These data indicate that the mutant virus growth rate is also affected in secondary tissues, impacting its ability to cross the salivary gland barriers and thus contributing to deficient transmission of the virus.

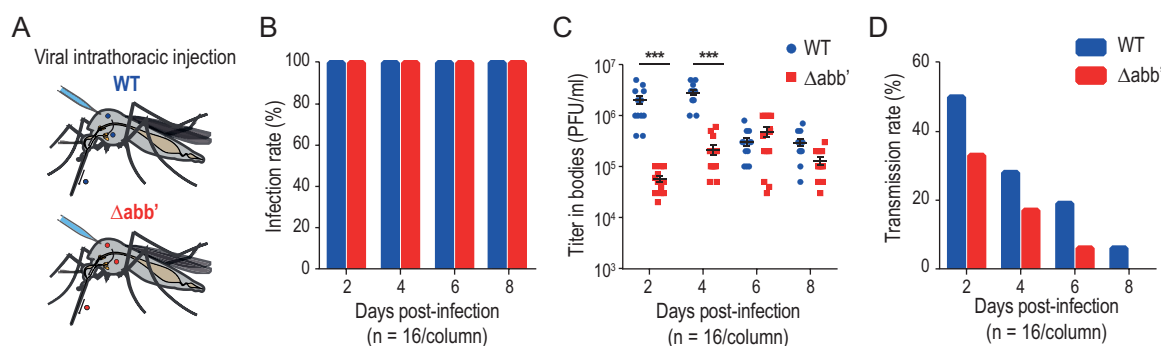


FIG 4 Salivary glands impose a tight barrier to CHIKV transmission. (A) Intrathoracic injections of *A. aegypti* mosquitoes with wild-type (WT) and $\Delta abb'$ CHIKVs. In order to bypass the midgut barrier, *A. aegypti* mosquitoes were intrathoracically injected with 2,500 PFU of WT or mutant virus. (B) Bar graph showing infection rates in bodies after intrathoracic injection of viruses. The infection rate was calculated as the percentage of mosquitoes with virus presence in the body at different times postinjection. (C) Dot plot showing mean viral titers and SD in the bodies of intrathoracically injected mosquitoes. For the viral titers, statistics were performed by a Mann-Whitney U test. (D) Bar graph showing transmission rates after intrathoracic injection of viruses. The transmission rate was calculated as the percentage of mosquitoes with virus presence in the saliva at different times postinjection.

Wild-type CHIKV displays a fitness advantage to escape from the mosquito midgut. To directly address the impact of the CHIKV growth rate on fitness, we performed competition experiments between wild-type and $\Delta abb'$ viruses. *A. aegypti* mosquitoes were fed with an infectious blood meal containing 10^6 PFU/ml of a mixture of wild-type and $\Delta abb'$ viruses in a 1:10 ratio in order to give a quantitative advantage to the virus with the impaired phenotype (Fig. 5A). At different times after the blood meal, total RNA was purified from individual mosquitoes and subjected to reverse transcription (RT) reactions with an oligo(dT) primer. The pool of viral cDNAs was used to amplify viral 3' UTRs, which yielded fragments of different lengths for the wild-type and mutant viruses. The gel in Fig. 5B shows the amplification products of wild-type and mutant viruses in a 1:10 ratio in the input used for the blood meal (amplification products of the wild-type and the $\Delta abb'$ 3' UTRs were used as a reference). The relative abundance of viruses with a full-length or $\Delta abb'$ 3' UTR was assessed by agarose gel electrophoresis analysis of the RT-PCR products amplified from individual mosquitoes 2, 5, and 9 days after feeding (Fig. 5C). The gels show the fragments amplified from 12 individual mosquitoes at each time point. For each lane, we scored the ratio of the intensities of the bands corresponding to the wild-type and mutant 3' UTRs and plotted the average ratio for each time point (Fig. 5D). The 1:10 ratio in the input was quickly reversed to a 1:1 ratio at the earliest time point evaluated. This rapid displacement of $\Delta abb'$ by wild-type virus *in vivo* indicates a fitness advantage of the wild-type virus during mosquito infections.

We next assessed whether the fitness advantage of the wild type reflected the observed differences in the abilities of the wild-type and mutant viruses to cross the midgut escape barrier. To this end, *A. aegypti* mosquitoes were fed with a blood meal containing a mixture of both viruses at a 1:1 ratio (Fig. 5B). The midgut and carcass were dissected at different time points, total RNA was extracted, and the presence of virus was evaluated by RT-PCR (Fig. 5E). Representative agarose gels of the midgut and carcass from day 4 postinfection illustrate the differential mobilities of wild-type and $\Delta abb'$ 3'-UTR amplification products (Fig. 5F). When analyzing the presence of viruses as a function of time, we observed that both viruses were detected in all mosquito midguts even at 8 days postinfection (Fig. 5G, top). Based on previous reports, we reasoned that incoming viruses likely formed independent foci of infection within the midgut and thus coexisted independently of their growth rates (24, 26, 34, 35). Wild-type virus was readily detected as of 2 days postinfection in the carcasses, while the mutant virus was detected only after 8 days, indicating that the wild type had a higher dissemination rate than the mutant virus at all times postinfection (Fig. 5G, bottom). Altogether, our experiments demonstrate that wild-type CHIKV has a fitness

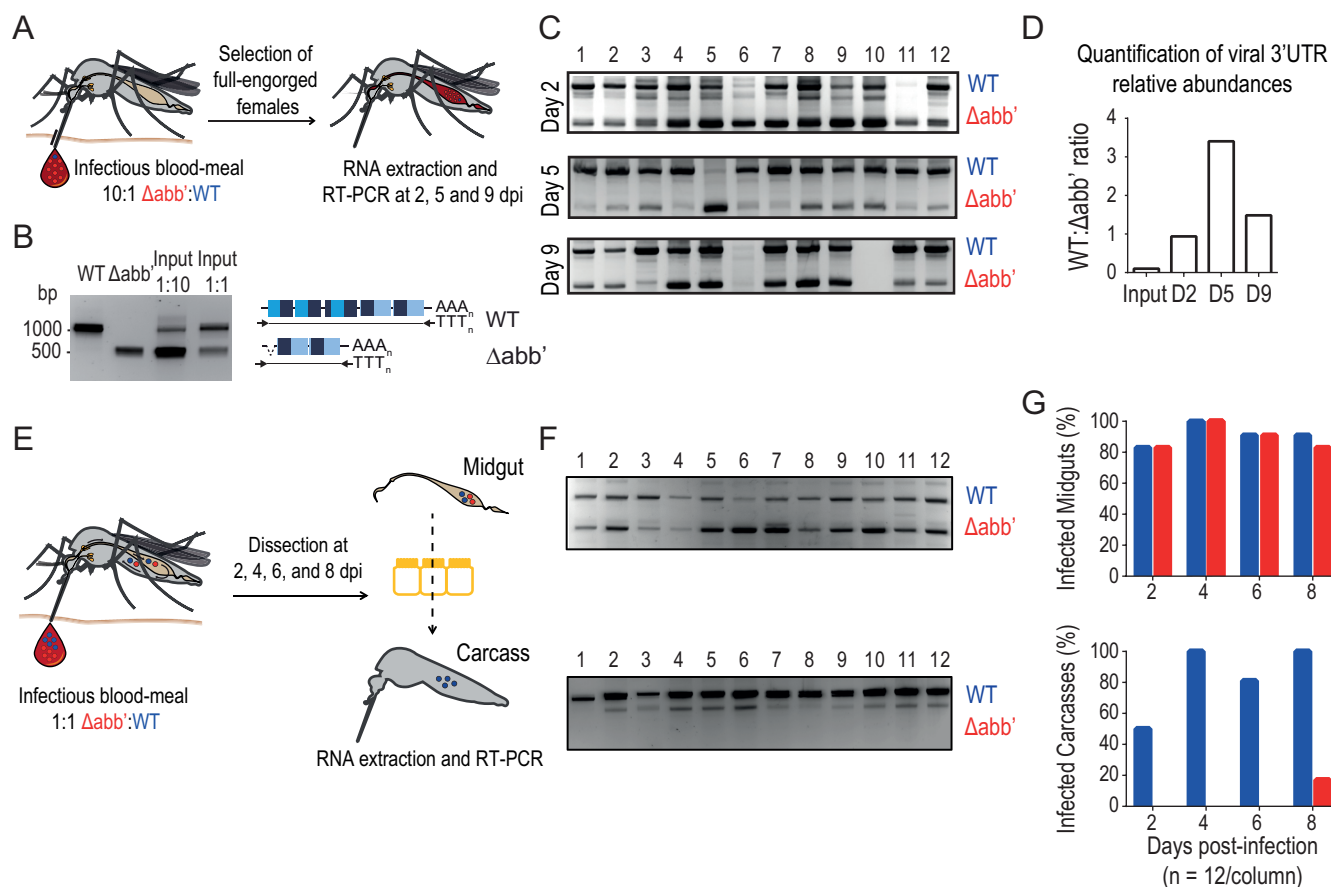


FIG 5 Wild-type CHIKV has a fitness advantage over $\Delta abb'$ CHIKV to cross the midgut escape barrier. (A) Experimental setup of wild-type (WT) versus $\Delta abb'$ competitions in *Aedes aegypti* mosquitoes. Mosquitoes were offered an infectious blood meal containing a mixture of WT and $\Delta abb'$ viruses in a 1:10 ratio (10^6 PFU/ml). Total RNA was purified from individual mosquitoes at different time points postinfection, and the presence of WT and $\Delta abb'$ 3' UTRs was assessed. (B) The RT-PCR product of the RNA extracted from the infectious blood meal containing wild-type and $\Delta abb'$ viruses in 1:1 and 1:10 ratios was resolved alongside fragments corresponding to wild-type and $\Delta abb'$ 3' UTRs for reference. (C) Agarose gel electrophoresis of 3'-UTR amplification products from individual mosquitoes. The presence of WT and $\Delta abb'$ viruses was assessed by RT-PCR and agarose gel electrophoresis on 12 individual mosquitoes at three different times after the blood meal. (D) Bar graph showing the ratio of WT to $\Delta abb'$ 3' UTRs in the input and in mosquito individuals during the time course of the experiment. Bars represent the average ratios of intensities for the bands corresponding to the products of amplification of WT and $\Delta abb'$ 3' UTRs in individual mosquitoes at each time point. (E) Competition assays to assess the ability of WT and $\Delta abb'$ CHIKVs to cross the midgut escape barrier. Infectious blood feeding of *A. aegypti* mosquitoes was performed with blood containing a mixture of both viruses at a 1:1 ratio (10^6 PFU/ml). At different times postinfection, the midgut and carcass were dissected, total RNA was extracted, and the presence of virus was evaluated by RT-PCR as described above. (F) Representative agarose gels showing the products of amplification from midgut (top) and carcass (bottom) samples of 12 individual mosquitoes at 4 days postinfection. (G, top) Bar graph showing the presence of WT and $\Delta abb'$ viruses in the midgut as a function of time. Bars represent the percentages of midguts where WT and $\Delta abb'$ viruses were detected. (Bottom) Bar graph showing the presence of WT and/or $\Delta abb'$ viruses in carcasses as a function of time. Bars represent the percentages of carcasses where WT and/or $\Delta abb'$ viruses were detected.

advantage over $\Delta abb'$ CHIKV due to a higher replication rate that enhances its ability to escape the midgut.

DISCUSSION

The infection kinetics of arboviruses in their mosquito vectors have long been recognized as a powerful determinant of transmission and epidemiology (29). Viral genetic variations influence growth kinetics and their interaction with mosquito barriers, which together contribute to the overall phenotype of virus transmission (23, 24, 36, 37). For instance, comparisons between dengue virus (DENV) serotypes and even between strains from single serotypes showed differences in EIPs that are most likely due to differences in viral replication kinetics in mosquitoes (29, 38). For CHIKV, the emergence of new viral lineages has been linked to large variations in the 3' UTR, which enhances replication in mosquito cells *in vitro* (15, 16, 18, 39, 40). Using an engineered 3'-UTR deletion mutant of the Caribbean lineage of CHIKV, we characterized the interaction of this mutant with mosquito barriers *in vivo*. We found that the replication

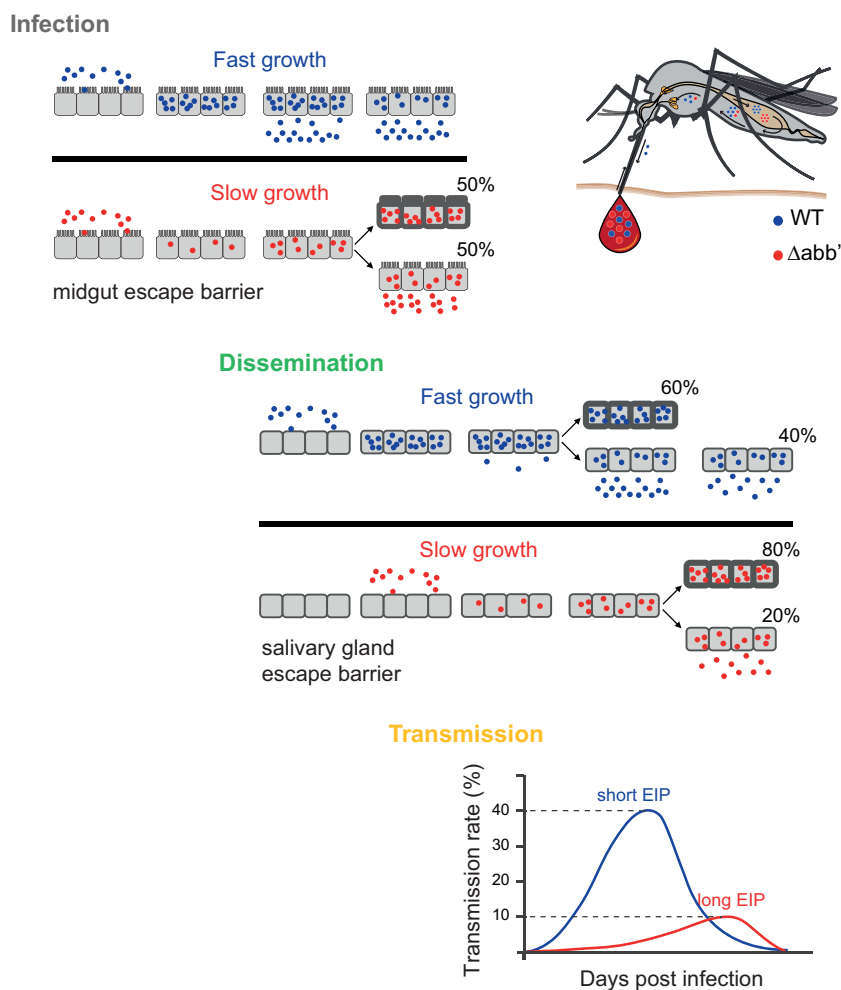


FIG 6 Model for the effect of the viral growth rate on the ability to cross barriers during the infectious cycle in mosquitoes. The infection rate in *Aedes* mosquitoes (midgut infection barrier) is almost 100%, regardless of the virus growth rate. Within midgut cells, wild-type (WT) CHIKV replicates and reaches the necessary threshold (>10,000 PFU) to cross the midgut escape barrier and spread into secondary tissues. A slow-growing virus accomplishes leaving the midgut at later times, and it spreads to secondary tissues in only 50% of individuals. WT disseminated viruses colonize the salivary glands and are successfully secreted into the saliva in 40% of individuals. Secretion into the saliva of mutant viruses is achieved in only 10% of mosquitoes with disseminated infection. The outcome is a longer EIP and a lower transmission efficiency of mutant (5%) than of WT (35%) CHIKV. After peaking (between 4 and 8 days postinfection for the WT and between 9 and 12 days postinfection for $\Delta abb'$), the transmission efficiency drops to undetectable levels.

rate of the 3'-UTR mutant is compromised in *Aedes* mosquitoes, and based on our results, we propose a model (Fig. 6) where the viral replication rate is intimately linked to the viral capacity to overcome barriers within mosquitoes. Viruses with high replication rates efficiently infect mosquitoes, disseminate to secondary tissues, and reach the mosquito saliva, resulting in a short EIP that ensures transmission. In contrast, viruses with low replication rates experience hurdles to overcoming the barriers imposed by the mosquitoes, resulting in a longer EIP and a lower transmission rate.

Important bottlenecks have been reported for arboviruses such as West Nile virus, Western equine encephalitis virus, Sindbis virus, and CHIKV during infection of their natural vectors (26, 33, 34, 41–43). These bottlenecks have been found at the midgut level and/or at the salivary gland level. By assessing viral infection rates in the midgut and carcass, we found that although there were no differences in the infectivity rates of both viral variants, the mutant virus had an impaired ability to leave the midgut, suggesting a strong midgut escape barrier effect. The outcome is a proportion of the

mosquito population exhibiting dissemination and the rest exhibiting no dissemination. This scenario of mosquito subpopulation structure has already been reported for DENV (38). In turn, a dose-dependent effect has also been associated with escape from the midgut and occurred only when low doses of virus had been ingested (24). In agreement, in this work, we found that increasing blood meal viral titers reduced the midgut escape barrier effect.

Once midgut infection has been established, in order to disseminate, the virus must cross the basal lamina surrounding the midgut epithelium. It has been shown that after a blood meal, both an alteration of the expression of specific enzymes in the mosquito midgut as well as mechanical distention occur (32, 44–46). Several works have proposed that this results in transient degradation and increased permissibility of the basal lamina, promoting a “window of opportunity” of 48 h during which large quantities of CHIKV are allowed to disseminate (32, 44). In this sense, viruses with longer mosquito replication cycles, such as DENV or Zika virus (ZIKV), may not benefit as much from the early transient degradation of the basal lamina following a blood meal (23). Interestingly, recent work has demonstrated that the acquisition of a second noninfectious blood meal significantly shortens the EIP of all these viruses in infected *Aedes* mosquitoes by triggering mechanical distention in the basal lamina and thus enhancing virus dissemination from the mosquito midgut (46). Our results suggest that CHIKV may need to reach threshold viral titers within midgut cells that are necessary but not sufficient to cross the midgut escape barrier and spread into secondary tissues. We speculate that the Δ abb' CHIKV mutant may miss that window of opportunity because it does not reach the threshold titers required to disseminate at early times after infection. Whether the administration of a second blood meal with the mutant virus has a positive effect on dissemination as a consequence of the mechanical distention of the basal lamina remains to be tested. Altogether, our data indicate that the low replication rate of the 3'-UTR mutant has a strong effect on the ability of CHIKV to escape the midgut at the onset of infection.

It is well established that selective pressures in the mosquito vector impose important population bottlenecks to arboviruses (23, 36, 37, 47). Given that the viral infection cycle in mosquitoes moves in a stepwise fashion, selective pressures in an initial tissue might have effects on the viral kinetics in downstream tissues (38, 48). CHIKV replication in mammalian cells was previously shown to generate virus variants with shorter 3' UTRs, including large deletions of direct repeat elements similar to the engineered mutation evaluated here (18). Furthermore, viruses with shorter 3' UTRs seemingly display a replicative advantage in mammalian cells. Similar to previous work (16), by using virus competitions in mosquitoes coinfecting with wild-type and mutant viruses, we observed a displacement of the mutant virus by the wild-type virus. In addition, we found that this fitness advantage is due to an increased capacity to escape from the midgut to secondary tissues, which results in a shift in the composition of the viral population. Interestingly, both viruses were simultaneously detected in the midguts of most of the mosquitoes even at 8 days postinfection. This suggests that coinfecting viruses formed independent foci of infection within the midgut, allowing both viruses to coexist independently of their replication rates (24, 26, 34, 35). These results widen the notion of how intrahost diversity plays a role in transmission, with variants with a fitness advantage spreading faster and eventually displacing those with lower fitness (38, 49). Epidemiological consequences might also be possible, like the 2008 large outbreak of dengue in Australia that was attributed to the very short EIP of the DENV3 strain in the mosquito (50). In nature, a significant proportion of mosquitoes are expected to die before they are capable of transmitting virus, and in this scenario, a virus variant with a shorter EIP would confer an evolutionary advantage by increasing its probability of transmission (5, 29, 51).

Taken together, our results show that a precisely timed replication rate is required for CHIKV to reach the necessary threshold titers to exit the midgut during the onset of the infection cycle, indicating that the viral replication rate is a determining factor in the ability to cross anatomical barriers and complete a successful replication cycle in

mosquitoes. Understanding the factors that affect viral trajectories between mosquito infection and viral transmission will help to predict viral epidemic potential and design strategies to disrupt the viral transmission cycle.

MATERIALS AND METHODS

Cells and viruses. Mammalian BHK and Vero cells were grown at 37°C in Dulbecco's modified Eagle's medium (DMEM) supplemented with 10% fetal bovine serum (FBS; Gibco) and 1% penicillin-streptomycin (Gibco). Mosquito C6/36 (*Aedes albopictus*) (ATCC CRL-1660) cells were grown at 28°C in Leibovitz L-15 medium supplemented with 10% FBS, 1% nonessential amino acids (Gibco), 2% tryptose phosphate broth (Sigma), and 1% penicillin-streptomycin. For RNA transfections, cell lines were grown to 60 to 70% confluence and transfected in 24-well plates using Lipofectamine 3000 (Invitrogen) according to the manufacturer's instructions. Caribbean wild-type and Δ abb' infectious clones were obtained as described previously (18). Viral stocks were obtained by transfection of 500 ng of *in vitro*-transcribed viral RNA and harvested from the cell culture supernatant at different times posttransfection. Viruses were quantified by plaque assays. To this end, 10⁵ Vero cells per well were seeded into 24-well plates and allowed to attach overnight. Viral stocks were serially diluted, 0.1 ml was added to the cells, and the mixture was incubated for 1 h. Next, 1 ml of an overlay (1× DMEM, 2% fetal bovine serum, 1% penicillin-streptomycin, and 0.8% agarose) was added to each well. Cells were fixed 3 days after infection with 4% paraformaldehyde and stained with crystal violet.

Mosquito rearing. Laboratory colonies of *A. aegypti* mosquitoes (17th generation; collected originally in Kamphaeng Phet Province, Thailand) and *A. albopictus* (19th generation; collected originally in Phu Hoa, Binh Duong Province, Vietnam) were used. The insectary conditions for mosquito maintenance were 28°C, 70% relative humidity, and a 12-h-light and 12-h-dark cycle. Adults were maintained with permanent access to a 10% sucrose solution. Adult females were offered commercial rabbit blood (BCL, Boisset-Saint-Priest, France) twice a week through a membrane feeding system (Hemotek Ltd.).

Experimental infections of mosquitoes. (i) Infectious blood meals. Infection assays were performed with 7- to 10-day-old females starved 24 h prior to infection in a biosafety level 3 (BSL-3) laboratory. Mosquitoes were offered the infectious blood meal for 30 min through a membrane feeding system (Hemotek Ltd.) set at 37°C with a piece of desalted pig intestine as the membrane. The blood meal was composed of washed human erythrocytes resuspended in phosphate-buffered saline mixed 2:1 with a prediluted viral stock and supplemented with 10 mM ATP (Sigma-Aldrich). The viral stock was prediluted in Leibovitz L-15 medium with 0.1% sodium bicarbonate (Gibco) to reach an infectious titer ranging from 1×10^6 to 1×10^7 focus-forming units and back-titrated to ensure similar presented doses (the exact titer of each infectious blood meal is noted for each experiment). Following the blood meal, fully engorged females were selected and incubated at 28°C with 70% relative humidity and under a 12-h-light and 12-h-dark cycle with permanent access to 10% sucrose. At different times postinfection, mosquitoes were cold anesthetized for salivation and dissection. For saliva collection, wings and legs were removed from each individual, and its proboscis was inserted into a 20- μ l tip containing 10 μ l of FBS for 30 min at room temperature. Saliva-containing FBS was expelled in 90 μ l of Leibovitz L-15 medium (Gibco) for amplification and titration. Following the collection of saliva, mosquitoes were dissected, and body parts were homogenized in microtubes containing steel beads (5-mm diameter) and 300 μ l of DMEM supplemented with 2% FBS using a TissueLyser II instrument (Qiagen) at 30 shakes/s for 2 min. Homogenates were clarified by centrifugation and stored at 80°C until further processing. Viral titers in individual samples were determined by plaque assays. For the detection of 3'-UTR RNA from whole mosquitoes or mosquito parts, RNA TRIzol extracted from homogenates was used for reverse transcription using reverse oligonucleotide 5'-TTTTTTTTTTTTTTTGAATAT-3', complementary to the poly(A) tail plus the last 7 nucleotides of CHIKV genomes. PCRs were then carried out (DreamTaq; Thermo Fisher) using the same reverse oligonucleotide and forward oligonucleotide 5'-CTAATCGTGGTGCTATG C-3'. The length of the viral 3' UTRs was estimated by resolving the product in 1% agarose gels. The intensity of the bands was measured with ImageJ software.

(ii) Intrathoracic inoculations of mosquitoes. Seven- to ten-day-old female mosquitoes were cold anesthetized and injected with a transfection mix of CellFectin II reagent (Thermo Fisher) with 50 nl of Leibovitz L-15 medium containing 2.5×10^3 PFU of virus. The injection was performed intrathoracically using a nanoinjector (Nanoject III; Drummond Scientific) and a glass capillary needle. At 2, 4, 6, and 8 days postinjection, mosquitoes were cold anesthetized and dissected.

Virus titration and quantification. The presence of infectious virus particles in mosquito bodies, midguts, carcasses, and head extracts was determined by plaque assays in homogenate samples following mosquito dissection. Briefly, 100 μ l of the sample homogenates was serially diluted in cell culture medium and used to infect Vero cells in 24-well plates as described above for virus titration. Mosquito saliva samples were amplified in C6/36 cells for 5 days, and virus presence in amplified supernatants was assessed by cytopathic effect in Vero cells. The data were analyzed quantitatively for most of the samples (PFU per milliliter) and qualitatively for saliva samples and some body and head samples (i.e., the presence or absence of infectious virus in heads/bodies). The infection rate (IR) was calculated as the proportion of mosquitoes infected among all tested females. The dissemination rate (DR) was defined as the proportion of females with infected head tissues among those that were infected (i.e., in which the virus successfully disseminated from the midgut). The dissemination efficiency (DE) was calculated as the proportion of females with infected head tissues among all tested females. The transmission rate (TR) was defined as the proportion of females with infectious saliva among those that developed a disseminated infection. The transmission efficiency (TE) was calculated as the overall

proportion of females that had infectious saliva (i.e., among all tested females with or without a disseminated infection).

Human blood and ethics statement. Human blood used to feed mosquitoes was obtained from healthy volunteer donors. Healthy donor recruitment was organized by local investigator assessment using medical history, laboratory results, and clinical examinations. Biological samples were supplied through the participation of healthy volunteers at the ICAREB biobanking platform (BB-0033-00062/ICAREB platform/Institut Pasteur, Paris/BBMRI AO203 [Bioresource]) of the Institut Pasteur for the CoSImmGen and Diamicoll protocols, which have been approved by the French Ethical Committee (CPP), Ile-de-France I. The Diamicoll protocol was declared to the French Research Ministry under reference number DC 2008-68 COL 1.

Statistics. All statistical analyses were performed in GraphPad Prism 6. Significant differences between virus infection, dissemination, and transmission rates were determined by Fisher's exact test. For viral titers, where the data did not follow a Gaussian distribution, a Mann-Whitney U test was used to replace the *t* test. Statistical significance is represented in the figures (*, $P \leq 0.05$; **, $P \leq 0.01$; ***, $P \leq 0.001$; ****, $P \leq 0.0001$).

ACKNOWLEDGMENTS

This work was supported by the European Research Council (FP7/2013-2019 ERC CoG 615220) and the French Government's Investissement d'Avenir program, Laboratoire d'Excellence Integrative Biology of Emerging Infectious Diseases (grant ANR-10-LABX-62-IBEID), to M.C.-S. F.M. was supported by a fellowship of the Argentine National Council for Scientific and Technical Research (CONICET). D.E.A. and C.V.F. are members of the CONICET.

REFERENCES

- Jones R, Kulkarni MA, Davidson TMV, RADAM-LAC Research Team, Talbot B. 2020. Arbovirus vectors of epidemiological concern in the Americas: a scoping review of entomological studies on Zika, dengue and chikungunya virus vectors. *PLoS One* 15:e0220753. <https://doi.org/10.1371/journal.pone.0220753>.
- Thaikruea L, Charearnsook O, Reanphumkarnkit S, Dissomboon P, Phonjan R, Ratchbud S, Kounsang Y, Buranapiyawong D. 1997. Chikungunya in Thailand: a re-emerging disease? *Southeast Asian J Trop Med Public Health* 28:359–364.
- Lanciotti RS, Valadere AM. 2014. Transcontinental movement of Asian genotype chikungunya virus. *Emerg Infect Dis* 20:1400–1402. <https://doi.org/10.3201/eid2008.140268>.
- Weaver SC. 2014. Arrival of chikungunya virus in the New World: prospects for spread and impact on public health. *PLoS Negl Trop Dis* 8:e2921. <https://doi.org/10.1371/journal.pntd.0002921>.
- Fredericks AC, Fernandez-Sesma A. 2014. The burden of dengue and chikungunya worldwide: implications for the southern United States and California. *Ann Glob Health* 80:466–475. <https://doi.org/10.1016/j.aogh.2015.02.006>.
- Mariconti M, Obadia T, Mousson L, Malacrida A, Gasperi G, Failloux A-B, Yen P-S. 2019. Estimating the risk of arbovirus transmission in Southern Europe using vector competence data. *Sci Rep* 9:17852. <https://doi.org/10.1038/s41598-019-54395-5>.
- Elsinga J, Grobusch MP, Tami A, Gerstenbluth I, Bailey A. 2017. Health-related impact on quality of life and coping strategies for chikungunya: a qualitative study in Curaçao. *PLoS Negl Trop Dis* 11:e0005987. <https://doi.org/10.1371/journal.pntd.0005987>.
- Hossain MS, Hasan MM, Islam MS, Islam S, Mozaffar M, Khan MAS, Ahmed N, Akhtar W, Chowdhury S, Arafat SMY, Khaleque MA, Khan ZJ, Dipta TF, Asna SMZH, Hossain MA, Aziz KS, Al Mosabbir A, Raheem E. 2018. Chikungunya outbreak (2017) in Bangladesh: clinical profile, economic impact and quality of life during the acute phase of the disease. *PLoS Negl Trop Dis* 12:e0006561. <https://doi.org/10.1371/journal.pntd.0006561>.
- Soumahoro M-K, Boelle P-Y, Gaüzere B-A, Atsou K, Pelat C, Lambert B, La Roche G, Gastellu-Etchegorry M, Renault P, Sarazin M, Yazdanpanah Y, Flahault A, Malvy D, Hanslik T. 2011. The chikungunya epidemic on La Réunion Island in 2005-2006: a cost-of-illness study. *PLoS Negl Trop Dis* 5:e1197. <https://doi.org/10.1371/journal.pntd.0001197>.
- Rezza G, Weaver SC. 2019. Chikungunya as a paradigm for emerging viral diseases: evaluating disease impact and hurdles to vaccine development. *PLoS Negl Trop Dis* 13:e0006919. <https://doi.org/10.1371/journal.pntd.0006919>.
- Achee NL, Grieco JP, Vatandoost H, Seixas G, Pinto J, Ching-Ng L, Martins AJ, Juntarajumnong W, Corbel V, Gouagna C, David J-P, Logan JG, Orsborne J, Marois E, Devine GJ, Vontas J. 2019. Alternative strategies for mosquito-borne arbovirus control. *PLoS Negl Trop Dis* 13:e0006822. <https://doi.org/10.1371/journal.pntd.0006822>.
- Tsetsarkin KA, Chen R, Weaver SC. 2016. Interspecies transmission and chikungunya virus emergence. *Curr Opin Virol* 16:143–150. <https://doi.org/10.1016/j.coviro.2016.02.007>.
- Pfeffer M, Kinney RM, Kaaden OR. 1998. The alphavirus 3'-nontranslated region: size heterogeneity and arrangement of repeated sequence elements. *Virology* 240:100–108. <https://doi.org/10.1006/viro.1997.8907>.
- Ou JH, Trent DW, Strauss JH. 1982. The 3'-non-coding regions of alphavirus RNAs contain repeating sequences. *J Mol Biol* 156:719–730. [https://doi.org/10.1016/0022-2836\(82\)90138-3](https://doi.org/10.1016/0022-2836(82)90138-3).
- Stapleford KA, Moratorio G, Henningsson R, Chen R, Matheus S, Enfissi A, Weissglas-Volkov D, Isakov O, Blanc H, Mounce BC, Dupont-Rouzeyrol M, Shomron N, Weaver S, Fontes M, Rousset D, Vignuzzi M. 2016. Whole-genome sequencing analysis from the chikungunya virus Caribbean outbreak reveals novel evolutionary genomic elements. *PLoS Negl Trop Dis* 10:e0004402. <https://doi.org/10.1371/journal.pntd.0004402>.
- Chen R, Wang E, Tsetsarkin KA, Weaver SC. 2013. Chikungunya virus 3' untranslated region: adaptation to mosquitoes and a population bottleneck as major evolutionary forces. *PLoS Pathog* 9:e1003591. <https://doi.org/10.1371/journal.ppat.1003591>.
- Filomatori CV, Merwaiss F, Bardossy ES, Alvarez DE. 11 July 2020. Impact of alphavirus 3'UTR plasticity on mosquito transmission. *Semin Cell Dev Biol* <https://doi.org/10.1016/j.semcdb.2020.07.006>.
- Filomatori CV, Bardossy ES, Merwaiss F, Suzuki Y, Henrion A, Saleh MC, Alvarez DE. 2019. RNA recombination at chikungunya virus 3'UTR as an evolutionary mechanism that provides adaptability. *PLoS Pathog* 15:e1007706. <https://doi.org/10.1371/journal.ppat.1007706>.
- Pezzi L, Diallo M, Rosa-Freitas MG, Vega-Rua A, Ng LFP, Boyer S, Drexler JF, Vasilakis N, Lourenco-de-Oliveira R, Weaver SC, Kohl A, de Lamballerie X, Failloux A-B, GloPID-R Chikungunya, O'nyong-nyong and Mayaro Virus Working Group. 2020. GloPID-R report on chikungunya, o'nyong-nyong and Mayaro virus, part 5: entomological aspects. *Antiviral Res* 174:104670. <https://doi.org/10.1016/j.antiviral.2019.104670>.
- Schule PA. 1928. Dengue fever: transmission by *Aedes aegypti*. *Am J Trop Med Hyg* 51–58:203–213. <https://doi.org/10.4269/ajtmh.1928.s1-8.203>.
- Hardy JL, Houk EJ, Kramer LD, Reeves WC. 1983. Intrinsic factors affecting vector competence of mosquitoes for arboviruses. *Annu Rev Entomol* 28:229–262. <https://doi.org/10.1146/annurev.en.28.010183.001305>.
- Coffey LL, Failloux A-B, Weaver SC. 2014. Chikungunya virus-vector interactions. *Viruses* 6:4628–4663. <https://doi.org/10.3390/v6114628>.

23. Rückert C, Ebel GD. 2018. How do virus-mosquito interactions lead to viral emergence? *Trends Parasitol* 34:310–321. <https://doi.org/10.1016/j.pt.2017.12.004>.
24. Franz AWE, Kantor AM, Passarelli AL, Clem RJ. 2015. Tissue barriers to arbovirus infection in mosquitoes. *Viruses* 7:3741–3767. <https://doi.org/10.3390/v7072795>.
25. Robison A, Young MC, Byas AD, Rückert C, Ebel GD. 2020. Comparison of chikungunya virus and Zika virus replication and transmission dynamics in *Aedes aegypti* mosquitoes. *Am J Trop Med Hyg* 103:869–875. <https://doi.org/10.4269/ajtmh.20-0143>.
26. Dong S, Kantor AM, Lin J, Passarelli AL, Clem RJ, Franz AWE. 2016. Infection pattern and transmission potential of chikungunya virus in two New World laboratory-adapted *Aedes aegypti* strains. *Sci Rep* 6:24729. <https://doi.org/10.1038/srep24729>.
27. Vega-Rúa A, Zouache K, Girod R, Failloux A-B, Lourenço-de-Oliveira R. 2014. High level of vector competence of *Aedes aegypti* and *Aedes albopictus* from ten American countries as a crucial factor in the spread of chikungunya virus. *J Virol* 88:6294–6306. <https://doi.org/10.1128/JVI.00370-14>.
28. Delang L, Yen P-S, Vallet T, Vazeille M, Vignuzzi M, Failloux A-B. 2018. Differential transmission of antiviral drug-resistant chikungunya viruses by *Aedes* mosquitoes. *mSphere* 3:e00230-18. <https://doi.org/10.1128/mSphere.00230-18>.
29. Fontaine A, Lequime S, Moltini-Conclois I, Jiolle D, Leparç-Goffart I, Reiner RCJ, Lambrechts L. 2018. Epidemiological significance of dengue virus genetic variation in mosquito infection dynamics. *PLoS Pathog* 14:e1007187. <https://doi.org/10.1371/journal.ppat.1007187>.
30. Salazar MI, Richardson JH, Sánchez-Vargas I, Olson KE, Beaty BJ. 2007. Dengue virus type 2: replication and tropisms in orally infected *Aedes aegypti* mosquitoes. *BMC Microbiol* 7:9. <https://doi.org/10.1186/1471-2180-7-9>.
31. Alto BW, Wiggins K, Eastmond B, Velez D, Lounibos LP, Lord CC. 2017. Transmission risk of two chikungunya lineages by invasive mosquito vectors from Florida and the Dominican Republic. *PLoS Negl Trop Dis* 11:e0005724. <https://doi.org/10.1371/journal.pntd.0005724>.
32. Dong S, Balaraman V, Kantor AM, Lin J, Grant DG, Held NL, Franz AWE. 2017. Chikungunya virus dissemination from the midgut of *Aedes aegypti* is associated with temporal basal lamina degradation during bloodmeal digestion. *PLoS Negl Trop Dis* 11:e0005976. <https://doi.org/10.1371/journal.pntd.0005976>.
33. Kramer LD, Hardy JL, Presser SB, Houk EJ. 1981. Dissemination barriers for Western equine encephalomyelitis virus in *Culex tarsalis* infected after ingestion of low viral doses. *Am J Trop Med Hyg* 30:190–197. <https://doi.org/10.4269/ajtmh.1981.30.190>.
34. Myles KM, Piero DJ, Olson KE. 2004. Comparison of the transmission potential of two genetically distinct Sindbis viruses after oral infection of *Aedes aegypti* (Diptera: Culicidae). *J Med Entomol* 41:95–106. <https://doi.org/10.1603/0022-2585.41.1.95>.
35. Smith DR, Arrigo NC, Leal G, Muehlberger LE, Weaver SC. 2007. Infection and dissemination of Venezuelan equine encephalitis virus in the epidemic mosquito vector, *Aedes taeniorhynchus*. *Am J Trop Med Hyg* 77:176–187. <https://doi.org/10.4269/ajtmh.2007.77.176>.
36. Forrester NL, Coffey LL, Weaver SC. 2014. Arboviral bottlenecks and challenges to maintaining diversity and fitness during mosquito transmission. *Viruses* 6:3991–4004. <https://doi.org/10.3390/v6103991>.
37. Forrester NL, Guérbois M, Seymour RL, Spratt H, Weaver SC. 2012. Vector-borne transmission imposes a severe bottleneck on an RNA virus population. *PLoS Pathog* 8:e1002897. <https://doi.org/10.1371/journal.ppat.1002897>.
38. Novelo M, Hall MD, Pak D, Young PR, Holmes EC, McGraw EA. 2019. Intra-host growth kinetics of dengue virus in the mosquito *Aedes aegypti*. *PLoS Pathog* 15:e1008218. <https://doi.org/10.1371/journal.ppat.1008218>.
39. Morley VJ, Noval MG, Chen R, Weaver SC, Vignuzzi M, Stapleford KA, Turner PE. 2018. Chikungunya virus evolution following a large 3'UTR deletion results in host-specific molecular changes in protein-coding regions. *Virus Evol* 4:vey012. <https://doi.org/10.1093/ve/vey012>.
40. Hyde JL, Chen R, Trobaugh DW, Diamond MS, Weaver SC, Klimstra WB, Wilusz J. 2015. The 5' and 3' ends of alphavirus RNAs—non-coding is not non-functional. *Virus Res* 206:99–107. <https://doi.org/10.1016/j.virusres.2015.01.016>.
41. Khoo CCH, Piper J, Sanchez-Vargas I, Olson KE, Franz AWE. 2010. The RNA interference pathway affects midgut infection- and escape barriers for Sindbis virus in *Aedes aegypti*. *BMC Microbiol* 10:130. <https://doi.org/10.1186/1471-2180-10-130>.
42. Göertz GP, Fros JJ, Miesen P, Vogels CBF, van der Bent ML, Geertsema C, Koenraadt CJM, van Rij RP, van Oers MM, Pijlman GP. 2016. Noncoding subgenomic flavivirus RNA is processed by the mosquito RNA interference machinery and determines West Nile virus transmission by *Culex pipiens* mosquitoes. *J Virol* 90:10145–10159. <https://doi.org/10.1128/JVI.00930-16>.
43. Grubaugh ND, Fauver JR, Rückert C, Weger-Lucarelli J, García-Luna S, Murrieta RA, Gendernalik A, Smith DR, Brackney DE, Ebel GD. 2017. Mosquitoes transmit unique West Nile virus populations during each feeding episode. *Cell Rep* 19:709–718. <https://doi.org/10.1016/j.celrep.2017.03.076>.
44. Kantor AM, Grant DG, Balaraman V, White TA, Franz AWE. 2018. Ultrastructural analysis of chikungunya virus dissemination from the midgut of the yellow fever mosquito, *Aedes aegypti*. *Viruses* 10:571. <https://doi.org/10.3390/v10100571>.
45. Cui Y, Grant DG, Lin J, Yu X, Franz AWE. 2019. Zika virus dissemination from the midgut of *Aedes aegypti* is facilitated by bloodmeal-mediated structural modification of the midgut basal lamina. *Viruses* 11:1056. <https://doi.org/10.3390/v11111056>.
46. Armstrong PM, Ehrlich HY, Magalhaes T, Miller MR, Conway PJ, Bransfield A, Misencik MJ, Gloria-Soria A, Warren JL, Andreadis TG, Shepard JJ, Foy BD, Pitzer VE, Brackney DE. 2020. Successive blood meals enhance virus dissemination within mosquitoes and increase transmission potential. *Nat Microbiol* 5:239–247. <https://doi.org/10.1038/s41564-019-0619-y>.
47. Lequime S, Fontaine A, Ar Gouilh M, Moltini-Conclois I, Lambrechts L. 2016. Genetic drift, purifying selection and vector genotype shape dengue virus intra-host genetic diversity in mosquitoes. *PLoS Genet* 12:e1006111. <https://doi.org/10.1371/journal.pgen.1006111>.
48. Hall MD, Bento G, Ebert D. 2017. The evolutionary consequences of stepwise infection processes. *Trends Ecol Evol* 32:612–623. <https://doi.org/10.1016/j.tree.2017.05.009>.
49. Lambrechts L, Fansiri T, Pongsiri A, Thaisomboonsuk B, Klungthong C, Richardson JH, Ponlawat A, Jarman RG, Scott TW. 2012. Dengue-1 virus clade replacement in Thailand associated with enhanced mosquito transmission. *J Virol* 86:1853–1861. <https://doi.org/10.1128/JVI.06458-11>.
50. Ritchie SA, Pyke AT, Hall-Mendelin S, Day A, Mores CN, Christofferson RC, Gubler DJ, Bennett SN, van den Hurk AF. 2013. An explosive epidemic of DENV-3 in Cairns, Australia. *PLoS One* 8:e68137. <https://doi.org/10.1371/journal.pone.0068137>.
51. Anderson JR, Rico-Hesse R. 2006. *Aedes aegypti* vectorial capacity is determined by the infecting genotype of dengue virus. *Am J Trop Med Hyg* 75:886–892. <https://doi.org/10.4269/ajtmh.2006.75.886>.